Globally Stable Feedback Laws for Near-Minimum-Fuel and Near-Minimum-Time Pointing Maneuvers for a Landmark-Tracking Spacecraft

Hanspeter Schaub, Rush D. Robinett and John L. Junkins

Simulated Reprint from

Journal of the Astronautical Sciences

Vol. 44, No. 4, Oct.–Dec. 1996, Pages 443-466

A publication of the
American Astronautical Society
AAS Publications Office
P.O. Box 28130
San Diego, CA 92198

AAS 95-417

GLOBALLY STABLE FEEDBACK LAWS FOR NEAR-MINIMUM-FUEL AND NEAR-MINIMUM-TIME POINTING MANEUVERS FOR A LANDMARK-TRACKING SPACECRAFT

Hanspeter Schaub[*], Rush D. Robinett[†] and John L. Junkins[‡]

Utilizing unique properties of a recently developed set of attitude parameters, the modified Rodrigues parameters, a feedforward/feedback type control laws is developed for a spacecraft undergoing large nonlinear motions using three reaction wheels. The method is suitable for tracking given reference trajectories that spline smoothly into a target state; these reference trajectories may be exact or approximate solutions of the system equations of motion. An associated asymptotically stable nonlinear observer is formulated for state estimation. In particular, we illustrate the ideas using both near-minimum-time and near-minimum fuel rotations about Euler's principal rotation axis, with parameterization of the sharpness of the control switching for each class of reference maneuvers. Lyapunov stability theory is used to prove rigorous global asymptotic stability of the closed-loop tracking error dynamics in the absence of external torques. If external torques are present, then the system is Lagrange stable. The methodology is illustrated by designing example control laws for a prototype landmark tracking spacecraft; simulations are reported that show this approach to be attractive for practical applications. The inputs to the reference trajectory are designed with user-controlled sharpness of all control switches, to enhance the trackability of the reference maneuvers in the presence of structural flexibility.

INTRODUCTION

Motivated by problems arising in the precision pointing of imaging satellites for non-proliferation and environmental monitoring applications, there is renewed interest in the problem of rapid large angle maneuvers followed by precision pointing/tracking of landmarks from near-earth orbits. Pointing and tracking tolerances for these imaging systems are on the order of microradians. There are many contributors to pointing error, but the vibrational disturbances induced by the effects of rapid maneuvers on flexible solar array structures are one major problem. In previous studies[1,2] it has been shown that, assuming sufficient sensor and actuator bandwidth, reaction wheel actuators can effectively control both the rigid body maneuvers and fine-pointing/vibration arrest; however, the key issue is to perform the large maneuvers in a torque-shaped fashion that minimizes disturbances of the flexural motion. Judicious torque shaping must be coupled with stabilizing feedback control to null tracking and fine pointing errors; this is the approach pursued herein. We seek to extend the developments of Ref. 1,2 to establish a globally asymptotically stable nonlinear control design approach of broad applicability to general three-dimensional pointing and tracking problems.

* Graduate Research Assistant, Aerospace Engineering Department, Texas A&M University, College Station TX 77843.

† Research Engineer at Sandia National Laboratories, Albuquerque, NM 87185.

‡ George Eppright Chair, Professor of Aerospace Engineering, Aerospace Engineering Department, Texas A&M University, College Station TX 77843, Fellow AAS.

In recent papers[3-9], the utility of a new set of orientation parameters (the modified Rodrigues parameters, MRPs) has been studied. It has been shown that these parameters have some outstanding properties. They appear to be the canonical three parameter set, owing to the following remarkable truths:

- The nonsingular motion range encompasses ±360 degrees, although the norm of the parameters tend to infinity as ±360 degrees rotations about any axis is approached.
- For rotations within ±180 degrees about any axis, the parameters are bounded by a norm of +1.
- The kinematic differential equations are quadratic nonlinear functions of the MRPs, and have no singular points for rotations less than ±360 degrees.
- The transformation from orthogonal components of angular velocity to the time derivatives of the MRPs involves a coefficient matrix with orthogonal rows and columns, thus the inverse is analytic.
- The MRPs are non unique, there are two trajectories corresponding exactly to a given physical motion. One of the trajectories at any instant of time lies within and the other lies outside a unit sphere. Both trajectories satisfy the same differential equations, only differing in initial conditions.

Regarding the last property, it is easy to establish the transformation between the corresponding points on the two trajectories, and this fact can be utilized to establish, for the first time, a globally nonsingular three parameter description of a generally tumbling rigid body.

These properties, together with recent results from Lyapunov control law design methods[1,2], enable the formulation of a most attractive and effective family of control laws for spacecraft attitude maneuvers and fine pointing. The control law design methodology is important in its own right, as distinct from the use of the MRPs as orientation coordinates. In particular, however, this control law design approach is especially attractive for this coordinate choice. The feedback law is dominated by linear terms for this approach with a judicious choice of a logarithmic Lyapunov function[5]. The analytical results presented herein are illustrated through a simulation study which supports the efficacy and practicality of the concepts introduced.

FORMULATION

The Equations Of Motion For A Rigid Spacecraft

The spacecraft is assumed to have three reaction wheels with distinct inertia aligned with the three body axes to control its attitude. Each reaction wheel inertia about the respective spin axis is given by J_i. Let the inertia matrix $\Im$ contain the spacecraft and the transverse reaction wheel inertia and let the matrix J be defined as

$$J = \begin{bmatrix} J_1 & 0 & 0 \\ 0 & J_2 & 0 \\ 0 & 0 & J_3 \end{bmatrix} \tag{1}$$

Let $\vec{\omega}_{B/N}$ be the spacecraft body angular velocity vector relative to an inertial frame N and let the $\vec{\Omega}$ vector contain the angular velocities of each reaction wheel. The rotational equations of motion can be written as[1]

$$\Im \frac{d\vec{\omega}_{B/N}}{dt} = -[\tilde{\omega}_{B/N}]\Im\vec{\omega}_{B/N} - [\tilde{\omega}_{B/N}]J(\vec{\Omega} + \vec{\omega}_{B/N}) - \vec{u} + \vec{f} \tag{2}$$

where the control vector $\vec{u}$ also satisfies the reaction axial wheel equation of motion:

$$\vec{u} = J\left(\frac{d\vec{\Omega}}{dt} + \frac{d\vec{\omega}_{B/N}}{dt}\right) \tag{3}$$

The tilde matrix $[\tilde{\omega}]$ is defined as

$$[\tilde{\omega}] = \begin{bmatrix} 0 & -\omega_3 & \omega_2 \\ \omega_3 & 0 & -\omega_1 \\ -\omega_2 & \omega_1 & 0 \end{bmatrix} \tag{4}$$

and the vector $\vec{f}$ is the sum of all external torques acting on the spacecraft. These torques are in part due to aerodynamic and solar radiation drag and are usually considered to be very small compared to the internal torques being applied.

Attitude Coordinates

All spacecraft orientations are described using sets of modified Rodrigues parameters[4-9]. They are a minimal coordinate representation of a rigid body attitude with several useful attributes. They can be defined in terms of the Euler parameters (quaternions) as

$$\sigma_i = \frac{\beta_i}{1+\beta_0} \qquad i = 1,2,3 \tag{5}$$

or in terms of the principal rotation axis $\hat{e}$ and the principal rotation angle ϕ as

$$\vec{\sigma} = \hat{e} \cdot \tan \phi/4 \tag{6}$$

Obviously they go singular at a principal rotation of ±360° where $\beta_0 \rightarrow -1$. What makes this set very attractive is that this singularity can be completely avoided by making use of the fact that the modified Rodrigues parameters are not unique. Notice that reversing the sign of the β's in Eq. (5) generates a second set of σ's. The alternate set is called the "shadow set"[4], and goes singular at zero rotations and is very well behaved around the ±360° rotations. Hence, if a singularity is approached with the original set, one can switch the attitude description to the "shadow set" and avoid the singularity at the cost of having a discontinuity at the switching point. The transformation between "original" and "shadow" set is[4,6]

$$\sigma_i^S = -\sigma_i \big/ \vec{\sigma}^T \vec{\sigma} \qquad i = 1,2,3 \tag{7}$$

Keep in mind that the choice in distinguishing "original" and "shadow" sets is purely arbitrary. Both sets describe the same physical orientation. In this study the switching condition was chosen to be $\vec{\sigma}^T \vec{\sigma} = 1$. This causes the magnitude of the orientation vector to be bounded between $0 \leq |\vec{\sigma}| \leq 1$. In terms of a principal orientation angle this means that the angle is restricted to be within $-180° \leq \phi \leq +180°$. Note that this combined set of "original" and "shadow" parameters implicitly "knows" the shortest way back to the origin[4]. Lengthy principal rotations of more than 180° are avoided. This will be useful when designing a robust attitude feedback control law. Also note from Eq. (6) that for the range $-180° \leq \phi \leq +180°$ the modified Rodrigues parameters behave very linearly. The differential kinematic equation of motion in terms of the modified Rodrigues parameters is given below[4,5]. Note that the equation only contains second order polynomial nonlinearities in $\vec{\sigma}$.

$$\frac{d\vec{\sigma}}{dt} = \frac{1}{2}\left[I\left(\frac{1-\vec{\sigma}^T\vec{\sigma}}{2}\right) + [\tilde{\sigma}] + \vec{\sigma}\vec{\sigma}^T \right]\vec{\omega} \tag{8}$$

Eq. (8) holds for both the "original" and the "shadow" set. This means that the derivative is well defined even at the switching point. The direction cosine matrix in term of the modified Rodrigues parameters is[4,5]

$$C(\vec{\sigma}) = \frac{1}{\left(1+\vec{\sigma}^T\vec{\sigma}\right)^2} \begin{bmatrix} 4\left(\sigma_1^2 - \sigma_2^2 - \sigma_3^2\right) + \Sigma^2 & 8\sigma_1\sigma_2 + 4\sigma_3\Sigma & 8\sigma_1\sigma_3 - 4\sigma_2\Sigma \\ 8\sigma_1\sigma_2 - 4\sigma_3\Sigma & 4\left(-\sigma_1^2 + \sigma_2^2 - \sigma_3^2\right) + \Sigma^2 & 8\sigma_2\sigma_3 + 4\sigma_1\Sigma \\ 8\sigma_1\sigma_3 + 4\sigma_2\Sigma & 8\sigma_2\sigma_3 + 4\sigma_1\Sigma & 4\left(-\sigma_1^2 - \sigma_2^2 + \sigma_3^2\right) + \Sigma^2 \end{bmatrix} \tag{9}$$

$$\Sigma = 1 - \vec{\sigma}^T\vec{\sigma}$$

OPEN-LOOP DYNAMICS

Rest-to-Rest Principal Rotation Reference Maneuver

Instead of doing a computationally expensive optimal control, all maneuvers performed will be about the *principal axis of rotation*. This will allow real-time pre-computation of the reference maneuvers. This solution is close to the optimal solution and *much* faster to compute. Euler's principal rotation theorem states that any reference frame can be related to another reference frame through a single-axis rotation. This theorem allows any three-dimensional rotation to be viewed as a single-axis rotation about the principal axis, as illustrated by the simple *one-dimensional* equation shown below.

$$\Im\ddot{\theta} = u \tag{10}$$

While certain gyroscopic coupling nonlinearities must be accounted for, since the actual motion will be fully three-dimensional, Eq. (10) provides a simple approach to design a reference trajectory. Let N denote the inertial and R denote the open-loop reference frames. The initial and final reference attitude can be established by the initial and final direction cosine matrices $[RN(t_0)]$ and $[RN(t_f)]$ in the sense

$$\vec{r}(t_f) = [RN(t_f)]\vec{n}(t_f), \qquad \vec{r}(t_0) = [RN(t_0)]\vec{n}(t_0) \tag{11a,b}$$

The rotation from the initial to the final position of the body axes is established by a direction cosine matrix $[RR(t_f, t_0)]$, where

$$\vec{r}(t_f) = [RR(t_f, t_0)]\vec{r}(t_0), \qquad [RR(t_f, t_0)] = [RN(t_f)][RN(t_0)]^T \tag{12a,b}$$

Euler's Principal axis of rotation is determined by finding the eigenvector of $[RR(t_f, t_0)]$ which corresponds to the eigenvalue +1; that is, we find the components $\{l_1, l_2, l_3\}$ of the unit vector satisfying

$$[RR(t_f, t_0)]\begin{Bmatrix} l_1 \\ l_2 \\ l_3 \end{Bmatrix} = \begin{Bmatrix} l_1 \\ l_2 \\ l_3 \end{Bmatrix} = \vec{l} \tag{13}$$

The principal rotation angle θ_f can be found by extracting the diagonal elements from the $[RR(t_f, t_0)]$ matrix[3]. We limit our principal rotation angles to be within $0° \le \theta \le 180°$, which is done automatically when using the inverse cosine function below.

$$\theta_f = \operatorname{acos}\left(\frac{trace([RR(t_f, t_0)]) - 1}{2}\right) \tag{14}$$

The principal axis of rotation can also be found[1], except near the zero and ±180° case, from the matrix elements of $[RR(t_f, t_0)]$.

$$\vec{l} = \frac{1}{2\sin\theta_f}\begin{Bmatrix} RR_{23} - RR_{32} \\ RR_{31} - RR_{13} \\ RR_{12} - RR_{21} \end{Bmatrix} \tag{15}$$

Taking the inverse kinematics viewpoint, we can prescribe a *reference trajectory* $\theta_r(t)$ as a rotation about the principal vector of $[RR(t_f, t_0)]$. For the reference trajectory to conform with the desired initial and final attitude, it is necessary that $\theta_r(t)$ satisfy the boundary conditions $\theta_r(0) = 0$ and $\theta_r(t_f) = \theta_f$.

Using the reference principal angle $\theta_r(t)$ and the principal axis of rotation $\vec{l}$, we can define the reference orientation, angular velocity and angular acceleration as

$$\vec{p}(t) = \vec{l} \cdot \tan\frac{\theta_r(t)}{4}, \qquad \vec{\omega}_r(t) = \vec{l}\,\dot{\theta}_r(t), \qquad \frac{d\vec{\omega}_r}{dt}(t) = \vec{l}\,\ddot{\theta}_r(t) \tag{16a,b,c}$$

where $\vec{p}(t)$ is a modified Rodrigues parameter vector which parameterizes the direction cosine matrix $\left[RR\left(t_f, t_0\right)\right]$. Given the above reference body angular velocity and acceleration and assuming no external torques, the reference control torque can be found using Eq. (2) with.

$$\vec{u}_r = -\Im \frac{d\vec{\omega}_r}{dt} - [\tilde{\omega}_r]\Im\vec{\omega}_r - [\tilde{\omega}_r]J\left(\vec{\Omega}_r + \vec{\omega}_r\right) \tag{17}$$

Near-Minimum-Time Maneuver

The optimal control for a rigid body minimum time maneuver is a "bang-bang" type control. For a rest-to-rest maneuver through a principal angle θ_f, the "bang-bang" control has the structure:

$$u(t) = u_{max} sign\left(t - \frac{t_f}{2}\right), \quad t_f = \sqrt{\frac{4\Im\theta_f}{u_{max}}} = \sqrt{\frac{4\theta_f}{\ddot{\theta}_{max}}}, \quad \ddot{\theta}_{max} = \frac{u_{max}}{\Im}$$

where $\ddot{\theta}_{max}$ and u_{max} are one-dimensional quantities measured along the principal axis of rotation.

If we anticipate that the "bang-bang" control will excite significant vibration of the flexible degrees of freedom, it is easy to smooth out the control switches using cubic splines and introduce "controllably sharp" torque switches using the smoothed "bang-bang" control shape[3]:

$$\ddot{\theta}_r(t) = \ddot{\theta}_{max} \begin{cases} \left(\frac{t}{\alpha t_f}\right)^2 \left(3 - 2\left(\frac{t}{\alpha t_f}\right)\right), & 0 \le t \le \alpha t_f \\ 1, & \alpha t_f \le t \le \frac{t_f}{2} - \alpha t_f \equiv t_1 \\ 1 - 2\left(\frac{t - t_1}{\alpha t_f}\right)^2 \left(3 - 2\left(\frac{t - t_1}{\alpha t_f}\right)\right), & t_1 \le t \le \frac{t_f}{2} + \alpha t_f \equiv t_2 \\ -1, & t_2 \le t \le t_f - \alpha t_f \equiv t_3 \\ -1 + \left(\frac{t - t_3}{\alpha t_f}\right)^2 \left(3 - 2\left(\frac{t - t_3}{\alpha t_f}\right)\right), & t_3 \le t \le t_f \end{cases} \tag{18}$$

where α controls the sharpness of the switches. $\alpha = 0$ generates the "bang-bang" instantaneous torque switches and $\alpha = 0.25$ generates the smoothest member of the family. After carrying out the double integration, the final maneuver time is found in terms of the principal angle rotated θ_f, the maximum principal angular acceleration $\ddot{\theta}_{max}$ and the smoothing factor α.

$$t_f = \sqrt{\frac{4\theta_f}{\ddot{\theta}_{max}} \cdot \frac{1}{1 - 2\alpha + \frac{2}{5}\alpha^2}}, \quad \ddot{\theta}_{max} = \frac{u_{max}}{\Im} \tag{19a,b}$$

The resulting principal angles and angular velocities can be seen in Figure 1, where $\alpha = 0.1$ was chosen. Obviously the maximum increase of maneuver time (for α =0.25) is less than 38%, compared to the "bang-bang" ($\alpha = 0$) case. For a flexible spacecraft, due to the decrease in vibrational energy, the actual maneuver time (including vibration settling time) is typically decreased significantly by using the smoothed "bang-bang" control. Even though we are not specifically considering the flexible spacecraft case at this point, we can implicitly consider flexibility by eliminating sharp torque switches which can be anticipated to "ring" the structure. Qualitatively, a sufficiently smooth and low amplitude torque history will make the most flexible structure behave more like a rigid structure and make the corresponding reference trajectory "more trackable." These statements can be made quite rigorously, see for example[1,2]. For well-chosen reference maneuvers and tracking law design, maneuver times for flexible spacecraft can usually be kept within 10 to 20% of the theoretical rigid body minimum maneuver times.

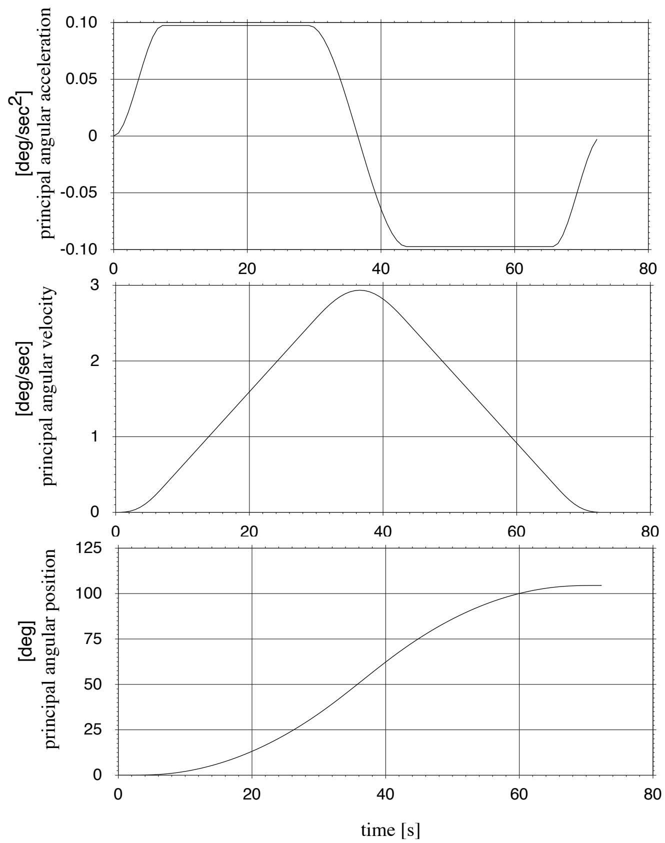

Figure 1 A Sample Torque Shaped Family of Near "Bang-Bang" Maneuvers

Near-Minimum-Fuel Maneuver

The torque time history of a optimal rigid body minimum-fuel maneuver consists of a sharp initial impulse to get the spacecraft rotating, a long coasting period, followed by a sharp reverse impulse to arrest the motion. Naturally, these sharp impulses would cause havoc for a highly flexible structure. Therefore a smoothed "bang-off-bang" control is chosen similar to the near-minimum-time maneuver presented previously.

$$\ddot{\theta}_r(t) = \ddot{\theta}_{max} \begin{cases} \left(\dfrac{t}{\alpha_1 t_f}\right)^2 \left(3 - 2\left(\dfrac{t}{\alpha_1 t_f}\right)\right), & 0 \le t \le \alpha_1 t_f \\ 1, & \alpha_1 t_f \le t \le \alpha_1 t_f + \alpha_2 t_f \equiv t_1 \\ \left(\dfrac{t_2 - t}{\alpha_1 t_f}\right)^2 \left(3 - 2\left(\dfrac{t_2 - t}{\alpha_1 t_f}\right)\right), & t_1 \le t \le 2\alpha_1 t_f + \alpha_2 t_f \equiv t_2 \\ 0, & t_2 \le t \le t_f - 2\alpha_1 t_f - \alpha_2 t_f \equiv t_3 \\ -\left(\dfrac{t - t_3}{\alpha_1 t_f}\right)^2 \left(3 - 2\left(\dfrac{t - t_3}{\alpha_1 t_f}\right)\right), & t_3 \le t \le t_f - \alpha_1 t_f - \alpha_2 t_f \equiv t_4 \\ -1, & t_4 \le t \le t_f - \alpha_1 t_f \equiv t_5 \\ -\left(\dfrac{t_f - t}{\alpha_1 t_f}\right)^2 \left(3 - 2\left(\dfrac{t_f - t}{\alpha_1 t_f}\right)\right), & t_5 \le t \le t_f \end{cases} \tag{20}$$

The instantaneous control switches are replaced by cubic splines with the rise and decay shape having controlled sharpness. Hence two torque smoothing factors α_1 and α_2 are used. The factor α_1 determines the rise or fall time from or to the maximum torque to zero torque as a percentage of the total maneuver time. The factor α_2 determines how long maximum torque is applied, also as a fraction of the total maneuver time. The amount of fuel used is chosen implicitly by specifying the two parameters α_1 and α_2 .

The total maneuver time for the smoothed "bang-off-bang" control is found again by twice integrating the one dimensional principal rotation equation.

$$t_f = \sqrt{\frac{4\theta_f}{\ddot{\theta}_{max}} \cdot \frac{1}{\alpha_1 + \alpha_2 - 2\alpha_1^2 - 3\alpha_1\alpha_2 - \alpha_2^2}}, \quad \ddot{\theta}_{max} = \frac{u_{max}}{\Im} \tag{21a,b}$$

The sample time history of principal angular acceleration, velocity and the principal angle for a smoothed "bang-off-bang" control is shown in Figure 2, where $\alpha_1 = \alpha_2 = 0.1$ were chosen.

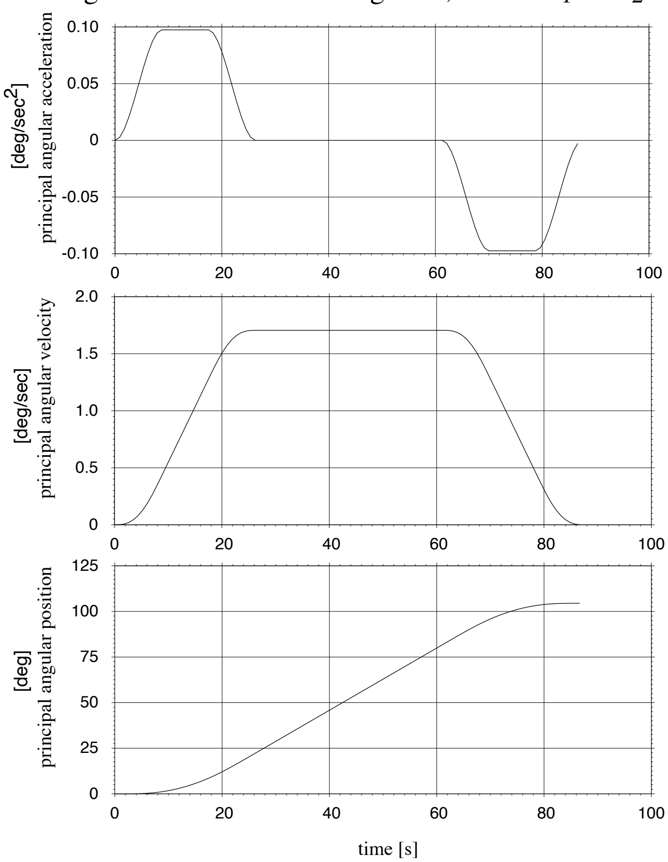

Figure 2 A Sample Torque-Shaped Family of Near "Bang-Off-Bang" Maneuvers

Incorporating Angular Velocity At The Final Maneuver Time

The principal rotation maneuver presented only applies to a rest-to-rest maneuver. To track a landmark, it is desired that the body have a certain angular velocity $\vec{\omega}(t_f)$ at the end of the maneuver. This allows the spacecraft to keep the sensors pointing toward a location on Earth for a finite duration of time and essentially achieve gross "motion compensation" for smear-free imaging. To accomplish this, the reference motion will be described relative to a moving target frame, not the inertial frame. Three coordinate frames are used:

R: open-loop reference coordinate axes (or follows the desired trajectory)

T: target motion coordinate frame

N: inertial coordinate frame

Let $\vec{\omega}_{T/N}$ be the body angular velocity vector of the target frame. In order to match up with our desired motion, the target frame T must have the following constraints.

$$\vec{\omega}_{T/N}(0) = 0 \qquad \vec{\omega}_{T/N}(t_f) = \vec{\omega}(t_f) \tag{22a,b}$$

$$[TN(t_f)] = [RN(t_f)] \tag{23}$$

Since the rest-to-rest principal rotation is described relative to the T frame, these conditions insure that the actual reference motion will have zero inertial angular velocity at *t=0*, and the desired orientation and angular velocity at the maneuver end.

Besides these three conditions any target motion can be chosen. The target motion used in this study was chosen to be a pure spin rotation about the $\vec{\omega}(t_f)$ axis, since an analytic solution exists for this trajectory. The orientation of the T frame at any time *t* is given as

$$[TN(t)] = [TT(t, t_f)][TN(t_f)] \tag{24}$$

where the matrix $[TT(t, t_f)]$ describes the pure spin motion away from the final target position. Let the modified Rodrigues parameter vector $\vec{p}_T$ parameterize the $[TT(t, t_f)]$ matrix with the condition that $\vec{p}_T(t_f) = 0$. The unit vector $\hat{l}_T$ is the principal axis of the target motion and is defined as

$$\hat{l}_T = \frac{\vec{\omega}(t_f)}{|\vec{\omega}(t_f)|} \tag{25}$$

and θ_T is the target principal rotation angle. The target motion $\vec{p}_T(t)$ is then defined as

$$\vec{p}_T(t) = \hat{l}_T \cdot \tan\frac{\theta_T}{4} \tag{26}$$

where $\theta_T(t_f) = 0$. To match initial and final conditions of the target angular velocity a cubic spline was used. By choice, this will result in the reference motion having no angular acceleration at the maneuver end, but this is not a requirement of the method itself. Any target angular velocity history that matches the conditions in Eqs. (22a,b) could have been used. The target angular velocity and acceleration are defined as:

$$\vec{\omega}_{T/N}(t) = |\vec{\omega}_{T/N}(t_f)| \left(\frac{t}{t_f}\right)^2 \left(3 - 2\frac{t}{t_f}\right) \cdot \hat{l}_T \tag{27}$$

$$\frac{d\vec{\omega}_{T/N}(t)}{dt} = \frac{|\vec{\omega}_{T/N}(t_f)|}{t_f} \left(6\frac{t}{t_f} - 6\left(\frac{t}{t_f}\right)^2\right) \cdot \hat{l}_T \tag{28}$$

After once integrating Eq. (27) the target principal rotation angle is found.

$$\theta_T(t) = \frac{|\vec{\omega}_{T/N}|}{t_f^2} \left(t^3 - \frac{t^4}{2t_f} - \frac{t_f^3}{2}\right) \qquad t_0 \le t \le t_f \tag{29}$$

The relative position of the reference frame to the target frame is given by the matrix $[RT(t)]$ which is found through

$$[RT(t)] = [RN(t)][TN(t)]^T \tag{30}$$

At the times t_0 and t_f the relative orientations are defined as

$$[RT(t_0)] = [RN(t_0)][TN(t_0)]^T \tag{31}$$

$$[RT(t_f)] = [RN(t_f)][TN(t_f)]^T = I \tag{32}$$

Eq. (12b) is now rewritten as

$$[RR(t_f, t_0)] = [RT(t_f)][RT(t_0)]^T = [RT(t_0)]^T \tag{33}$$

The matrix $[RR(t_f, t_0)]$ defined in Eq. (33) is used to define the rest-to-rest principal rotation motion for the case where the reference motion is supposed to have a final angular velocity.

Given the maneuver time t_f, we would be able to accurately describe the complete target motion. To find t_f though, we need to know the $[RR(t_f, t_0)]$ matrix first, which itself depends on the target motion. Since we only know the final, not the initial target position in advance, no closed form solution is available to find t_f. An iterative method was used to find the maneuver time. The initial estimate for t_f was found by assuming complete rest-to-rest motion. Using this t_f a new $[RR(t_f, t_0)]$ matrix was found and with it a new t_f. This method converged very quickly if half of the difference between old and new t_f was added to the old t_f.

The matrix $[RT(t)]$ is given as

$$[RT(t)] = [RR(t, t_0)][RT(t_0)] \tag{34}$$

where the $[RT(t_0)]$ matrix was defined in Eq. (31). The desired reference motion relative to the inertial frame is found from Eq. (30) to be

$$[RN(t)] = [RT(t)][TN(t)] \tag{35}$$

where the target motion $[TN(t)]$ is given in Eq. (24).

The angular velocity and acceleration expressed in Eq. (16b,c) are now expressed relative to the target frame motion. Hence, let us relabel these quantities as expressions relative to the target frame as

$$\vec{\omega}^R_{R/T}(t) = \vec{\omega}_r(t) \quad , \quad \frac{d\vec{\omega}^R_{R/T}(t)}{dt} = \frac{d\vec{\omega}_r(t)}{dt} \tag{36}$$

where the superscripts indicate in which coordinate frame the vectors are written. The reference angular velocity expressed relative to the inertial frame is given as

$$\vec{\omega}^R_{R/N} = \vec{\omega}^R_{R/T} + [RT]\vec{\omega}^T_{T/N} \tag{37}$$

To find the reference angular acceleration relative to the inertial frame, the inertial derivative of Eq. (37) is taken.

$$\begin{aligned} \frac{d}{dt}\left(\vec{\omega}^R_{R/N}\right)^N &= \frac{d}{dt}\left(\vec{\omega}^R_{R/N}\right)^R + [\tilde{\omega}_{R/N}]\vec{\omega}^R_{R/N} = \frac{d}{dt}\left(\vec{\omega}^R_{R/N}\right)^R \\ &= \frac{d\vec{\omega}^R_{R/T}}{dt} + [RT]\frac{d\vec{\omega}^T_{T/N}}{dt} - [\tilde{\omega}^R_{R/T}][RT]\vec{\omega}^T_{T/N} \end{aligned} \tag{38}$$

For the limiting case where the target frame has zero motion, Eqs. (37) and (38) collapse back to the rest-to-rest case given in Eqs. (16b,c).

CLOSED-LOOP DYNAMICS

Lyapunov Method To Design Nonlinear Tracking Control Law

A nonlinear tracking control law is developed to assure that the reference trajectory is asymptotically tracked in the absence of external torques. One advantage of this nonlinear control law over other control laws is that it is globally, asymptotically stabilizing assuming, of course that there are no modeling errors present. Secondly, through the choice of the attitude coordinates, this control law will bring a body, which has tumbled beyond ±180° from the reference motion, back to the reference trajectory through the shortest angular distance. The three coordinate frames used are:

B: actual spacecraft coordinate frame

R: reference coordinate axes

N: inertial coordinate frame

Let the [*BR*] matrix define the relative attitude of the spacecraft to the reference frame. It is related to [*BN(t)*] as

$$[BR] = [BN][RN]^T \tag{39}$$

Let the modified Rodrigues parameter vector $\vec{\sigma}$ parameterize the direction cosine matrix [*BR*]. This vector defines the orientation error of the spacecraft relative to the reference frame; achieving $\vec{\sigma} \rightarrow 0$ assumes asymptotic tracking of the reference motion. The extradition of the $\vec{\sigma}$ vector from the [*BR*] matrix is easily accomplished by use of the β_0 Euler parameter. The complete transformation is given below.

$$\begin{aligned} 2\beta_0 &= +\sqrt{trace([BR]) + 1} \\ \sigma_1 &= \frac{BR_{23} - BR_{32}}{4\beta_0(1 + \beta_0)} \\ \sigma_2 &= \frac{BR_{31} - BR_{13}}{4\beta_0(1 + \beta_0)} \\ \sigma_3 &= \frac{BR_{12} - BR_{21}}{4\beta_0(1 + \beta_0)} \end{aligned} \tag{40}$$

By assuring that $\beta_0 \geq 0$ we are guaranteed to have a modified Rodrigues vector[4] with $|\vec{\sigma}| \leq 1$. By using the modified Rodrigues parameters to describe the error in orientation, the feedback control law will inherently know the "shortest way" back to the reference frame. As an example, if the spacecraft has rotated a principal rotation of +200° off from the reference condition, the control law will know to let the spacecraft complete the rotation. It will perform a +160° principal rotation instead of a -200° maneuver, bringing the spacecraft back to the reference state "the short way round"[4].

Obviously, it is desired to make the body frame track the reference frame, and thus the objective of the tracking control law should be to make any departure motion $\vec{\sigma}$ vanish. Let all the following vectors be written in the body frame *B*, unless noted otherwise. The error in body angular velocity is given as

$$\delta\vec{\omega} = \vec{\omega}_{B/N} - [BR]\vec{\omega}^R_{R/N} \tag{41}$$

The reference body angular velocity vector must be transferred into the body frame, since it is only given in the reference frame *R*. The error in body angular acceleration is found by taking the derivative of Eq. (41).

$$\frac{d}{dt}(\delta\vec{\omega})^N = \frac{d}{dt}(\vec{\omega}_{B/N})^N - [BR]\frac{d}{dt}(\vec{\omega}_{R/N})^N + [\tilde{\omega}_{B/N}][BR]\vec{\omega}^R_{R/N} \tag{42}$$

The Lyapunov function for the feedback control law is defined to be

$$V = \frac{1}{2}\delta\vec{\omega}^T \Im \delta\vec{\omega} + 2K\log\left(1 + \vec{\sigma}^T\vec{\sigma}\right) \tag{43}$$

where *K* is a scalar gain for the attitude error feedback. Using the logarithm of the departure motion will result in a feedback control law which is linear in $\vec{\sigma}$ [4,5]. As Tsiotras points out in Ref. 5, this remarkable fact occurs because $d/dt\left(2\log\left(1 + \vec{\sigma}^T\vec{\sigma}\right)\right) = \delta\vec{\omega}^T\vec{\sigma}$ .To guarantee global asymptotic stability, let us verify that the first time derivative of *V* is negative definite.

$$\dot{V} = \delta\vec{\omega}^T \Im \frac{d}{dt}(\delta\vec{\omega})^N + K \cdot \delta\vec{\omega}^T\vec{\sigma} \tag{44}$$

Substituting Eqs. (42) and (2) into Eq. (44) yields

$$\dot{V} = \delta\vec{\omega}^T \Big(-[\tilde{\omega}_{B/N}]\Im\vec{\omega}_{B/N} - [\tilde{\omega}_{B/N}]J\big(\vec{\Omega} + \vec{\omega}_{B/N}\big) - \vec{u} + \vec{f} \\ - \Im[BR]\frac{d}{dt}(\vec{\omega}_{R/N})^N + \Im[\tilde{\omega}_{B/N}][BR]\vec{\omega}^R_{R/N} + K\vec{\sigma}\Big) \tag{45}$$

After defining the control torque vector $\vec{u}$ to be

$$\vec{u}^B = -\Im\Big([BR]\frac{d}{dt}\big(\vec{\omega}^R_{R/N}\big)^N - [\tilde{\omega}_{B/N}][BR]\vec{\omega}^R_{R/N}\Big) \\ - [\tilde{\omega}^B_{B/N}]\Im\vec{\omega}^B_{B/N} - [\tilde{\omega}^B_{B/N}]J\big(\vec{\Omega}^B + \vec{\omega}^B_{B/N}\big) + K\vec{\sigma}^B + P\delta\vec{\omega}^B \tag{46}$$

where the matrix P is a positive definite angular velocity feedback matrix. For clarity, all vectors were labeled with their corresponding coordinate frame. Note that the control torque is dominated by linear terms in the attitude error $\vec{\sigma}$ and the angular velocity error $\delta\vec{\omega}$. After substituting $\vec{u}$ into Eq. (45) $\dot{V}$ is shown to be

$$\dot{V} = -\delta\vec{\omega}^T P\delta\vec{\omega} + \delta\vec{\omega}^T\vec{f} \tag{47}$$

The above $\dot{V}$ does not guarantee any stability if external torques are present. All it says is that $\delta\vec{\omega}$ will remain bounded. After backsubstituting the control torque in Eq. (46) into the equations of motion and making some simplifications, the following closed loop error dynamics are found. Let the $'$ symbol represent the inertial derivative operator.

$$\delta\vec{\omega}' = -\Im^{-1}\big(K\vec{\sigma} + P\delta\vec{\omega} - \vec{f}\big) \tag{48}$$

$$\vec{\sigma}' = \frac{1}{2}\left[I\left(\frac{1-\vec{\sigma}^T\vec{\sigma}}{2}\right) + [\tilde{\sigma}] + \vec{\sigma}\vec{\sigma}^T\right]\delta\vec{\omega} = g(\vec{\sigma})\delta\vec{\omega} \tag{49}$$

The two first order differential equations can be combined into one second order equation. Assuming a constant external torque yields

$$\Im\delta\vec{\omega}'' + P\delta\vec{\omega}' + Kg(\vec{\sigma})\delta\vec{\omega} = \vec{f}' = 0 \tag{50}$$

Except for the $g(\vec{\sigma})$ term, this equations looks like the standard unforced vibration equation. Since $\vec{\sigma} \in L_\infty$ the function $g(\vec{\sigma})$ will be bounded. Because Eq. (50) has a positive damping term and $\delta\vec{\omega}$ remains bounded, $\delta\vec{\omega}''$ and $\delta\vec{\omega}'$ will decay to zero as time goes to infinity. The $\delta\vec{\omega}$ that the system will settle on is determined by

$$Kg(\vec{\sigma})\delta\vec{\omega}_\infty = 0 \tag{51}$$

Since the $g(\vec{\sigma})$ matrix is always invertible[6], $\delta\vec{\omega}_\infty$ will decay to the zero vector. To find the attitude tracking error, take the limit of Eq. (48) as time goes to infinity.

$$\lim_{t\to\infty}(\Im\delta\vec{\omega}') = \lim_{t\to\infty}\big(-K\vec{\sigma} - P\delta\vec{\omega} + \vec{f}\big) \tag{52}$$

Because the body angular velocity and acceleration error will decay to zero, the attitude error will converge to the finite offset

$$\lim_{t\to\infty}\vec{\sigma} = \frac{\vec{f}}{K} \tag{53}$$

Note that in the absence of external torques the attitude error decays to zero, making the tracking error dynamics globally asymptotically stable! In the presence of a disturbing external torque, the body angular velocity errors still decays to zero. However, the attitude will converge to a finite offset shown above, making the system Lagrange stable or bounded. Since the external torques encountered are typically very small, this attitude offset is usually also very small. I can be reduced by choosing a larger attitude feedback gain K or by implementing an adaptive update scheme to estimate and compensate for the actual external torque.

Control Feedback Gain Selection

Assuming zero external torques, the closed-loop dynamics are found by substituting Eqs. (2) and (42) into Eq. (46). The resulting differential equation only depends on the attitude error $\vec{\sigma}$ and the body angular velocity error $\delta\vec{\omega}$.

$$\frac{d}{dt}(\delta\vec{\omega})^N = -K\cdot\Im^{-1}\vec{\sigma} - \Im^{-1}P\delta\vec{\omega} \tag{54}$$

Note that the differential equation for $\delta\vec{\omega}$ is *linear* without making any approximations. The nonlinearity of the closed-loop dynamics come in through the coupling with $\vec{\sigma}$. If $\vec{\sigma} = 0$, then the poles of Eq. (54) could be chosen arbitrarily. The differential equation for $\vec{\sigma}$ depends quadratically on $\vec{\sigma}$. After linearizing Eq. (49) about $\vec{\sigma} = 0$, the following approximation is obtained

$$\frac{d\vec{\sigma}}{dt} \approx \frac{\delta\vec{\omega}}{4} \tag{55}$$

Remember that the modified Rodrigues parameters act like angles over four. This fact is visible again in the above approximation. Because of this, the linearization using modified Rodrigues parameters will be valid for twice the rotation range compared to the classical Rodrigues parameters, and four times the range over the most attractive set of Euler angles. After combining Eqs. (54) and (55), the following closed-loop error dynamics are found:

$$\begin{bmatrix} \frac{d}{dt}(\vec{\sigma})^N \\ \frac{d}{dt}(\delta\vec{\omega})^N \end{bmatrix} = \begin{bmatrix} 0 & \frac{1}{4}I \\ -K\cdot\Im^{-1} & -\Im^{-1}P \end{bmatrix} \begin{bmatrix} \vec{\sigma} \\ \delta\vec{\omega} \end{bmatrix} \tag{56}$$

Given an arbitrary inertia matrix $\Im$, a root-locus method could be used to find the poles of Eq. (56). The roots cannot be placed arbitrarily because K is only a scalar gain. If the inertia matrix $\Im$ and the angular velocity feedback matrix P are chosen to be diagonal matrices, then Eq. (56) can be decoupled into three sets of two equations

$$\begin{bmatrix} \dot{\sigma}_i \\ \delta\dot{\omega}_i \end{bmatrix} = \begin{bmatrix} 0 & \frac{1}{4} \\ -\frac{K}{\Im_i} & -\frac{p_i}{\Im_i} \end{bmatrix} \begin{bmatrix} \sigma_i \\ \delta\omega_i \end{bmatrix} \qquad i = 1,2,3 \tag{57}$$

whose roots can be solved explicitly as

$$\lambda = -\frac{1}{2}\left(\frac{p_i}{\Im_i} + \sqrt{-\frac{K}{\Im_i} + \left(\frac{p_i}{\Im_i}\right)^2}\right) \quad \textit{and} \quad \lambda = -\frac{1}{2}\left(\frac{p_i}{\Im_i} - \sqrt{-\frac{K}{\Im_i} + \left(\frac{p_i}{\Im_i}\right)^2}\right) \tag{58}$$

Note that the only approximations made in the above analysis are the linearization of Eq. (49) and the assumption of a diagonal inertia matrix $\Im$. Since the linearization of the modified Rodrigues parameters are valid for four times the rotational range of the Euler angles, and the off diagonal terms in the inertia matrix are usually very small compared to the diagonal terms, this linearization will typically predict the dynamics of the nonlinear system for moderately large tracking errors.

Figure 3 shows the root-locus plot of Eq. (58). A separate p_i can be chosen for each body axis, but only one attitude error feedback gain K can be chosen.

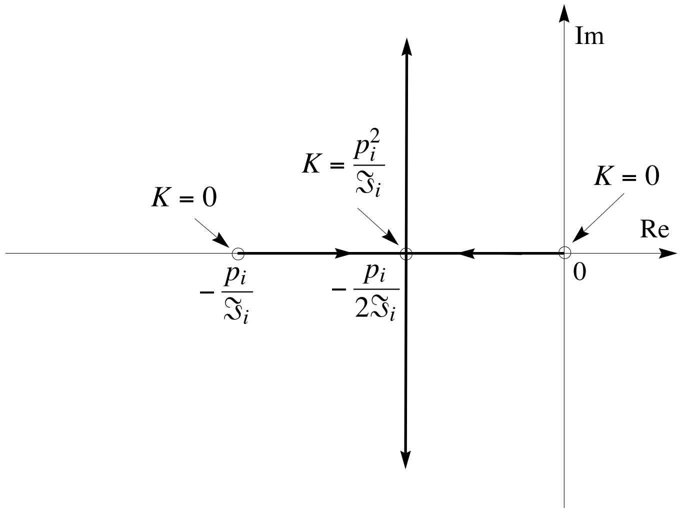

Figure 3 Root-Locus Plot of the Decoupled, Linearized Error Dynamics

Assuming that the closed-loop dynamics will be slightly under-damped, we can write the angular velocity feedback gains p_i in term of the controller decay time constants T_c .

$$p_i = 2\Im_i \frac{\ln 2}{T_c} \qquad i = 1, 2, 3 \tag{59}$$

The scalar attitude feedback gain K is still free to be chosen. For the close-loop dynamics to be under-damped, the condition on K is

$$K > \frac{p_i^2}{\Im_i} \qquad i = 1, 2, 3 \tag{60}$$

Note that both K and p_i determine whether the closed-loop dynamics are over-, critically-, or under-damped. But if the system is under-damped, then only p_i determines how fast a state error will decay. On the other hand, the gain K influences the frequency of the oscillations ω_{c_i} .

$$\omega_{c_i} = \frac{1}{2}\sqrt{\frac{K}{\Im_i} - \left(\frac{p_i}{\Im_i}\right)^2} \qquad K = \Im_i\left(\omega_{c_i}^2 + \left(\frac{p_i}{\Im_i}\right)^2\right) \qquad i = 1, 2, 3 \tag{61a,b}$$

To avoid reaction wheel saturation, a method of control gain scheduling would be used[10].

STATE ESTIMATION

The purpose of this nonlinear estimator is to cancel any measurements errors in the body attitude vector $\vec{q}$ (given in modified Rodrigues parameters) and the body angular velocity $\vec{\omega}$, even in the presence of an unmodeled external torque $\vec{f}$ and a gyro rate bias $\vec{b}$. Let the measured states be denoted as $\vec{X}_m$, the estimated states as $\vec{X}_{est}$ and the actual states as $\vec{X}$.

$$\vec{X}_m = \begin{bmatrix} \vec{q}_m \\ \vec{\omega}_m \\ \vec{b}_m \end{bmatrix} \qquad \vec{X}_{est} = \begin{bmatrix} \vec{q}_{est} \\ \vec{\omega}_{est} \\ \vec{b}_{est} \end{bmatrix} \qquad \vec{X} = \begin{bmatrix} \vec{q} \\ \vec{\omega} \\ \vec{b} \end{bmatrix} \tag{62}$$

The rate gyro bias $\vec{b}$ is assumed to be constant for small time intervals, thus having the following kinematic equation

$$\frac{d}{dt}(\vec{b}) = 0 \tag{63}$$

Let the estimator error be defined as

$$\vec{e} = \vec{X}_{est} - \vec{X} = \begin{bmatrix} \Delta\vec{q} \\ \Delta\vec{\omega} \\ \Delta\vec{b} \end{bmatrix} \quad (64)$$

From Eqs. (2,8,63), the actual system dynamics can be written as

$$\frac{d}{dt}(\vec{X}) = F(\vec{X}) - \begin{bmatrix} 0 \\ \Im^{-1}\vec{u} \\ 0 \end{bmatrix} + \begin{bmatrix} 0 \\ \vec{d} \\ 0 \end{bmatrix} \quad (65)$$

where the *F()* function contains the dynamical system. The angular acceleration $\vec{d}$ due to the unmodeled external torques is defined as

$$\vec{d} = \Im^{-1}\vec{f} \quad (66)$$

and is assumed to have a known bound $\vec{D}$ satisfying $\vec{D}_i \geq \vec{d}_i$. If the bounds of the rate gyro bias error $\Delta\vec{b}$ and of the angular acceleration due to external forces $\vec{d}$ are known, then the following dynamics of the estimated state scan be shown to be asymptotically stable for arbitrary large estimated state attitude and angular velocity errors.

$$\frac{d}{dt}(\vec{X}_{est}) = F\left(\vec{X}_m - \begin{bmatrix} 0 \\ \vec{b}_{est} \\ 0 \end{bmatrix}\right) - \begin{bmatrix} 0 \\ \Im^{-1}\vec{u} \\ 0 \end{bmatrix} - \begin{bmatrix} \vec{E}_{\vec{q}} \\ \vec{E}_{\vec{\omega}} \\ 0 \end{bmatrix} - H\left(\vec{X}_{est} - \vec{X}_m + \begin{bmatrix} 0 \\ \vec{b}_{est} \\ 0 \end{bmatrix}\right) \quad (67)$$

The estimator feedback gain matrix *H* is positive definite and partitioned as

$$J = \begin{bmatrix} H_{11} & H_{12} & H_{13} \\ H_{21} & H_{22} & H_{23} \\ H_{31} & H_{32} & H_{33} \end{bmatrix}$$

The vectors $\vec{E}_{\vec{q}}$ and $\vec{E}_{\vec{\omega}}$ are defined as[11]

$$[\vec{E}_{\vec{q}}]_i = \max\left(\text{abs}\left([H_{12}\Delta\vec{b}_{max}]_i\right)\right) \cdot \text{sgn}(\Delta\vec{q}_i) \quad (68)$$

$$[\vec{E}_{\vec{\omega}}]_i = \max\left(\text{abs}\left([H_{22}\Delta\vec{b}_{max}]_i\right) + \vec{D}_i\right) \cdot \text{sgn}(\Delta\vec{\omega}_i) \quad (69)$$

The asymptotic stability of Eq. (67) is proven with the Lyapunov function

$$V = \frac{1}{2}\vec{e}^T\vec{e} \quad (70)$$

Let the measured states be broken up into the true states, the random white noise $\vec{v}$ and the rate bias components.

$$\vec{X}_m = \vec{X} + \vec{v} + \begin{bmatrix} 0 \\ \vec{b} \\ 0 \end{bmatrix} \quad (71)$$

By enforcing the asymptotic stability requirement $\dot{V} < 0$ and by making use of Eqs. (64), (65) and (67), the following asymptotic stability condition is found.

$$\begin{aligned} &\vec{e}^T\left(F\left(\vec{X} + \vec{v} - \begin{bmatrix} 0 \\ \Delta\vec{b} \\ 0 \end{bmatrix}\right) - F(\vec{X}) + H\vec{v}\right) - \Delta\vec{q}^T\left(\vec{E}_{\vec{q}} + H_{12}\Delta\vec{b}\right) \\ &- \Delta\vec{\omega}^T\left(\vec{E}_{\vec{\omega}} + \vec{d} + H_{22}\Delta\vec{b}\right) - \Delta\vec{b}^T H_{33}\Delta\vec{b} < \vec{e}^T H\vec{e} \end{aligned} \quad (72)$$

Note that since *H* is positive definite, the right-hand side (RHS) of Eq. (72) will always be greater than zero for $\vec{e} \neq 0$. Assuming there is no measurement noise, no rate gyro bias and no unmodeled external torques, than the estimator dynamics in Eq. (67) is globally asymptotically stable. We offer the following qualitative observations regarding tuning of the estimator.

If an unmodeled external angular acceleration $\vec{d}$ is present with a known bound $\vec{D}$, then the estimator dynamics are still stable, since the $\Delta\vec{q}^T$ term of the left-hand side (LHS) is guaranteed to be negative definite by the definition of $\vec{E}_{\vec{q}}$. Stability is still guaranteed for any positive definite *H* and any estimated attitude and angular velocity errors.

If a rate bias $\vec{b}$ is introduced with a bounded error $\Delta\vec{b}$, then *H* can no longer be arbitrarily small. The first term of the LHS could be positive. The estimator feedback gain matrix *H* must be chosen large enough such that $\vec{e}^T H\vec{e}$ is always larger than the first term of the LHS. The second, third and fourth term of the LHS are guaranteed to be negative definite by the definition of $\vec{E}_{\vec{q}}$ and $\vec{E}_{\vec{\omega}}$, and because H_{33} is positive definite.

Once white measurement noise is introduced, the estimated states will not converge to the actual states of course, but will oscillate about them. While doing discrete sampling of the states at Δt intervals, the dominant noise term of the estimator dynamics is $H\vec{v}$. The actual jump due to noise from one sample to another is bounded by $H\vec{v}_{max}\Delta t$. To further adjust the filter characteristics, the sampling time interval can be tuned. The measurement noise also has a second degrading effect. It may cause the *sgn* functions in Eqs. (68,69) to return an incorrect sign of $\Delta\vec{q}_i$ and $\Delta\vec{\omega}_i$. This will cause a secondary noise induced effect of the estimated states between samples, of the order of $\vec{E}_{\vec{q}}\Delta t$ and $\vec{E}_{\vec{\omega}}\Delta t$ respectively. Again the filtering errors are controlled by choosing the sampling interval.

Under- and over-damped estimator dynamics were compared. For a given decay time constant, the over-damped system was better able to cancel measurement noise than the under-damped system. To assure that all the attitude and angular velocity measurement errors decay at the same rate, the estimator feedback matrix *H* was chosen to be of diagonal form.

$$H = \begin{bmatrix} H_{est} \cdot I & 0 & 0 \\ 0 & H_{est} \cdot I & 0 \\ 0 & 0 & H_{\vec{b}} \end{bmatrix} \tag{73}$$

Writing the estimator feedback gain H_{est} in terms of an estimator error decay time constant we get

$$H_{est} = \frac{\ln 2}{T_E} \tag{74}$$

The estimator feedback gain $H_{\vec{b}}$ can have a much larger decay time constant than H_{est}, since the rate gyro bias is assumed to change very slowly. Having a small $H_{\vec{b}}$ helps in reducing the secondary noise effect for the rate gyro bias estimation. In practice, we may use the above estimation algorithm to baseline a Kalman-Filter, or other linear state algorithm, appropriate for real-time on board implementation.

RESULTS

The following figures show the results of rigid body rotation simulation. The body inertia matrix $\Im$ has only diagonal entries of 200 kgm^2, 200 kgm^2 and 118 kgm^2 corresponding to the first, second and third body axis. The spacecraft has three reaction wheels aligned with the body axis whose inertia about the rotation axis are 0.00955 kgm^2, 0.1240 kgm^2 and 0.00955 kgm^2 respectively. The maneuver takes the spacecraft (in 3-2-1 Euler angles) from (-4°,-55°,4°) to (4°,55°,-4°). The rotation is mainly about the pitch axis with some slight yawing and rolling. The craft starts out with zero angular velocity and is required to have a final angular velocity of -1°/s about the pitch axis at the end of the maneuver. The error in initial attitude and angular velocity is (-0.05°,0.8°,0.05°) and (-0.025°/s,0.1°/s,0.025°/s).

The feedback control law was chosen to have a time constant T_c of 4 seconds and an attitude feedback gain *K* of 44. This results in the feedback response in the pitch and yaw axis having a damped frequency of 9.05 °/s, and the roll axis having damped frequency of 14.4 °/s. The estimator time constant T_E was set to be 0.4 seconds, an order of magnitude faster than T_c. The initial estimated 3-2-1 Euler angles were (-4.1°,-55.5°,3.95°). The attitude noise measurements were subjected to random noise of the magnitude of 4e-5 (given in MRP). The initial estimated body angular velocities were (-0.02°/s,0.15°/s,0.03°/s). The angular velocity measurement noise level was set to 5e-5 °/s.

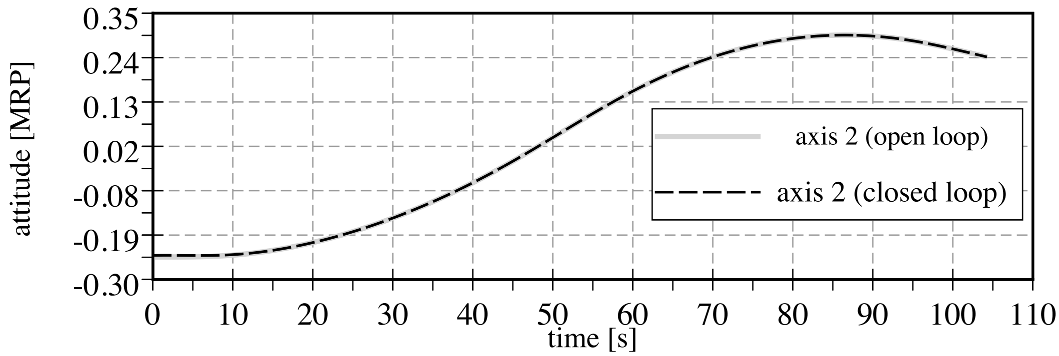

Figure 4 Open- and Closed-Loop Attitude for 2nd Body Axis

The total maneuver time was 104.09 seconds. Figures 4 and 5 show the attitude time history in MRP space. The closed-loop motion accurately tracks the open-loop trajectory. Figure 4 shows the large pitching maneuver. Since a final negative angular velocity is required about the 2nd body axis, the craft has to rotate beyond the target attitude and return to it with the desired angular velocity. The open-loop maneuver designed in this paper performs this task in a very smooth and near-optimum fashion.

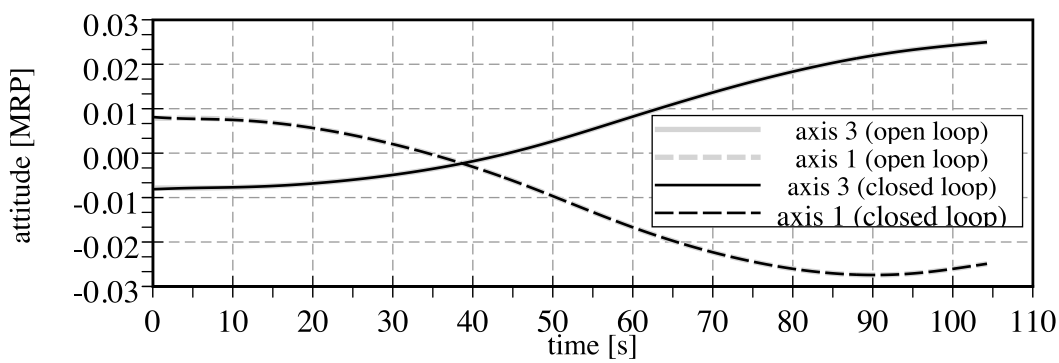

Figure 5 Open- and Closed-Loop Attitude for 1st and 3rd Body Axis

Figures 6 and 7 show the time history of the angular velocities. The open-loop maneuver correctly ends with a zero angular velocity about the 1st and 3rd body axis, and with -1°/s about the second body axis with no angular acceleration. If a final angular acceleration is required, this could easily be incorporated into the target trajectory used to generate the open-loop motion.

The initial state errors are canceled by the feedback control law and the open-loop trajectory is tracked accurately.

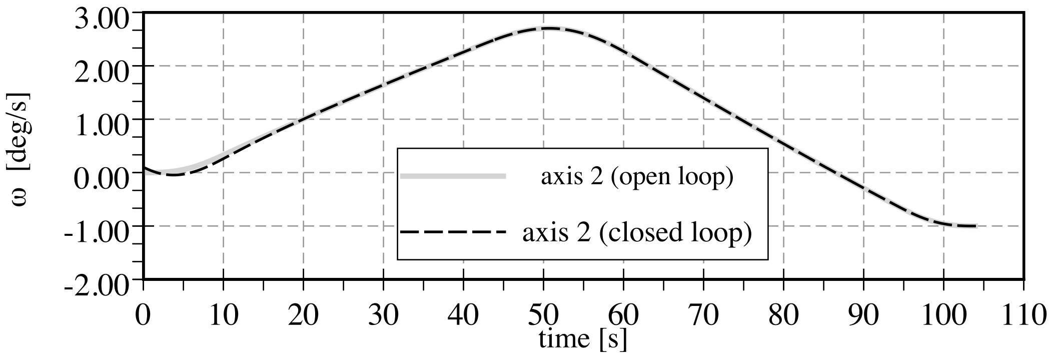

Figure 6 Open- and Closed-Loop Body Angular Velocity for 2nd Body Axis

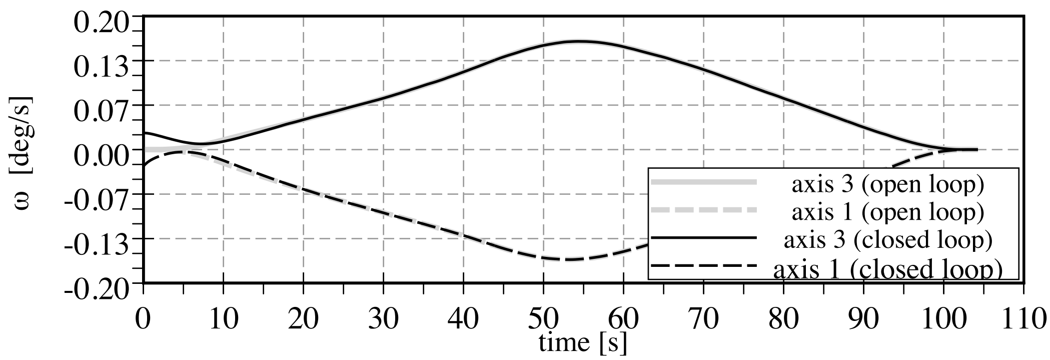

Figure 7 Open- and Closed-Loop Body Angular Velocity for 1st and 3rd Body Axis

Figures 8 and 9 show the time history of the internal control torque exerted onto the three reaction wheels. The maximum torque encountered is 0.3108 Nm by the second reaction wheel. The measurement noise is not visible in Figure 4 because of the relatively high torques. The closed-loop time history appears smooth and asymptotically approaches the open-loop torque.

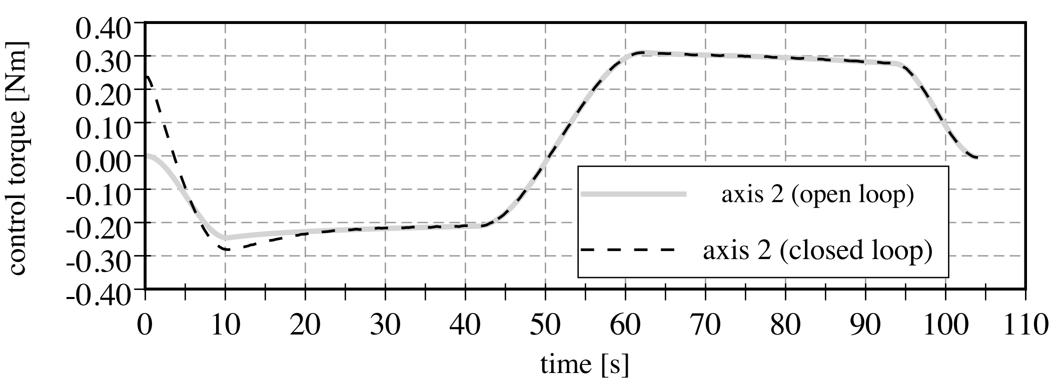

Figure 8 Open- and Closed-LoopControl Torque for 2nd Reaction Wheel

The measurement noise is visible for the 1st and 3rd reaction wheels, since they are only exerting relatively low torques. But even here the noise is small compared to the torques and does not pose any fine pointing problems. The closed-loop motion still asymptotically approaches the open-loop control torque.

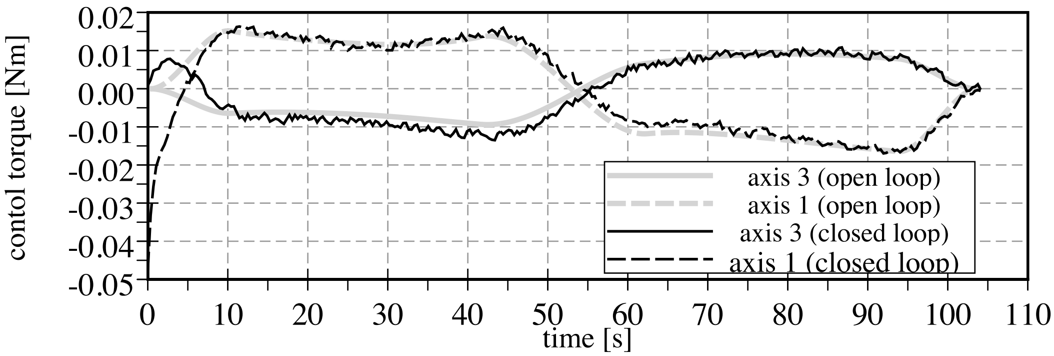

Figure 9 Open- and Closed-Loop Control Torque for 1st and 3rd Reaction Wheels

Figure 10 shows the time history of the attitude tracking error between the estimated states and the open-loop states. The linearization used to find the controller feedback gains very accurately models the actual nonlinear feedback dynamics. The decay time constants and the damped frequencies match with the simulation very well.

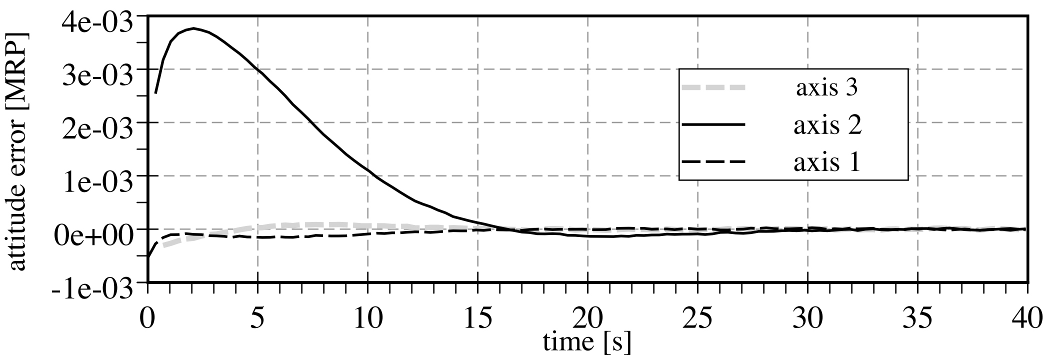

Figure 10 Closed-Loop Attitude Tracking Error

Figure 11 shows the time history of the angular velocity tracking error. Similar observations as with the attitude tracking error can be made. In both cases the initial state error is asymptotically canceled. The error is effectively gone after about 20 seconds. The measurement noise levels are too low to be visible on these figures.

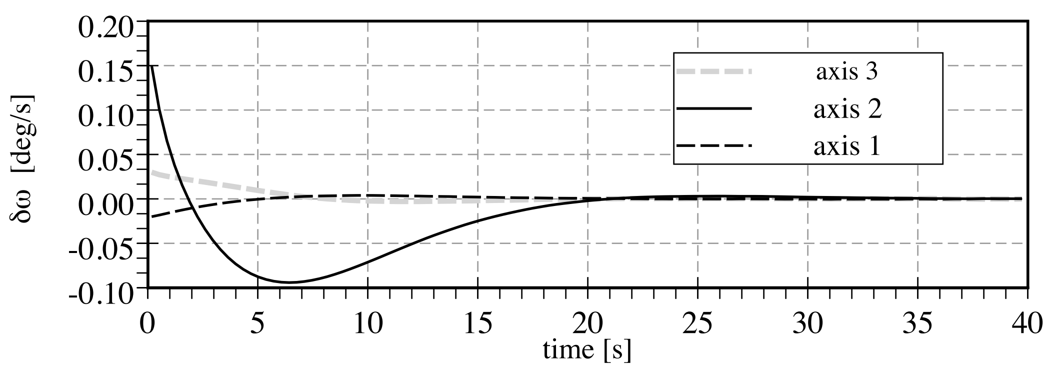

Figure 11 Closed-Loop Body Angular Velocity Tracking Error

Figures 12 and 13 show the time histories of the estimator tracking error between the estimated states and the actual states. Again the predicted estimator responses matches very well with the actual nonlinear response. The estimator dynamics are over-damped and errors decay an order of magnitude faster than the controller dynamics. The errors are effectively gone after about 2 seconds.

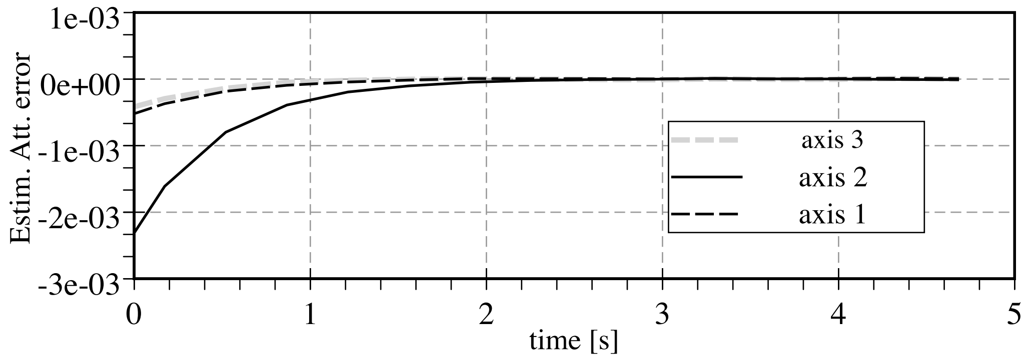

Figure 12 Estimator Attitude Tracking Error

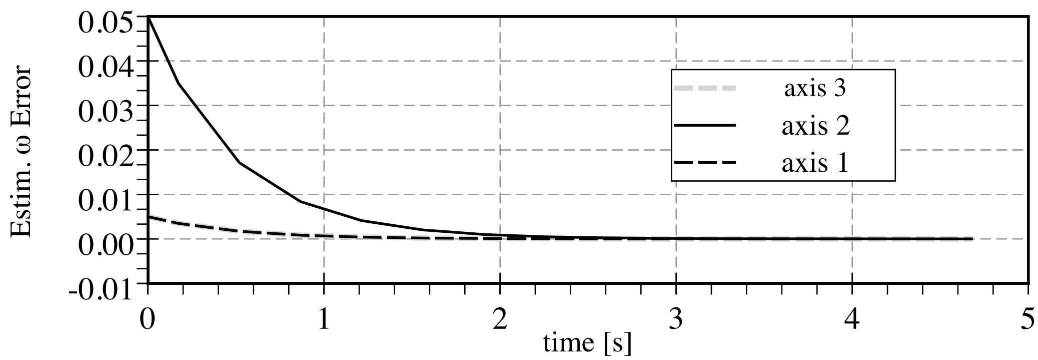

Figure 13 Estimator Body Angular Velocity Tracking Error

CONCLUSIONS

A nonlinear feedback control approach has been developed for large three-dimensional rotational maneuvers. A unique coordinate choice and the use of Lyapunov control design methods are the key new ingredients blended to produce these results. To avoid excessive "ringing" of the structure, the near-minimum-time and near-minimum-fuel reference control torques were smoothed with cubic splines.

The feedforward/feedback control law presented is globally asymptotically stable without, and Lagrange stable with bounded external torques. The nonlinear estimator has proven Lyapunov stability, and asymptotic stability in the absence of measurement noise. It is also able to compensate for unmodeled external torques and rate gyro biases.

The actual closed-loop controller and estimator feedback dynamics matched very well with the dynamics predicted in the feedback gain selection sections, since only the attitude dynamics had to be linearized. Because of the choice of attitude coordinates, the modified Rodrigues parameters, this linearization is valid for a range of attitude errors four times larger than if Euler angles were used, and two times larger than if the classical Rodrigues parameters were used.

The maneuver demonstrated was able to track the open-loop trajectory asymptotically and cancel any initial state or estimator errors.

REFERENCES

[1] Junkins, J. L., and Kim, Y., *Introduction to Dynamics and Control of Flexible Structures*, AIAA Education Series, Washington D.C., 1993.

[2] Junkins, J. L., Rahman, Z. H., and Bang, H., "Near-Minimum-Time Maneuvers of Distributed Parameter Systems: Analytical and Experimental Results," *Journal of Guidance, Control, and Dynamics*, Vol. 14, No. 2 (March-April, 1991), pp. 406-415.

[3] Junkins, J .L, and Turner, J. D., *Optimal Spacecraft Rotational Maneuvers*, Elsevier Science Publishers, Netherlands, 1986.

[4] Schaub, H., and Junkins, J. L., "Stereographic Orientation Parameters for Attitude Dynamics: A Generalization of the Rodrigues Parameters," AAS/AIAA Spaceflight Mechanics Meeting, Albuquerque, New Mexico, Feb. 13-16, 1995, paper AAS 95-137.

[5] Tsiotras, P. "New Control Laws for the Attitude Stabilization of Rigid Bodies," Proceedings, IFAC Symposium on Automatic Control in Aerospace, Palo Alto, CA, Sept. 12-16, 1994, pp. 316-321.

[6] Schaub, H., Tsiotras, P., and Junkins, J. L., "Principal Rotation Representations of Proper NxN Orthogonal Matrices," to appear in International Journal of Engineering Science, 1994.

[7] Marandi, S. R., and Modi, V. J., "A Preferred Coordinate System and the Associated Orientation Representation in Attitude Dynamics," *Acta Astronautica*, Vol. 15, 1987, pp. 833-843.

[8] Wiener, T. F., "Theoretical Analysis of Gimballess Inertial Reference Equipment Using Delta-Modulated Instruments," Diss. Massachusetts Institute of Technology, March 1962.

[9] Shuster, M. D., "A Survey of Attitude Representations," *Journal of the Astronautical Sciences*, Vol. 41, No. 4, 1993, pp. 439-517.

[10] Schaub, H., Robinett, R. D., and Junkins, J. L., "Globally Stable Feedback Laws for Near-Minimum-Fuel and Near-Minimum-Time Pointing Maneuvers for a Landmark Tracking Spacecraft," AAS/AIAA Astrodynamics Specialist Conference, Halifax, Nova Scotia, Canada, August 14-17, 1995, paper AAS 95-417.

[11] Cristi, R., Burl, J., and Russo, N., "Adaptive Quaternion Feedback Regulation for Eigenaxis Rotations," Department of Electrical and Computer Engineering, Naval Postgraduate School, Monterey, CA, June 1993.